Comparison of Magnetic Resonance Elastography and Diffusion-weighted Imaging for Staging Hepatic Fibrosis

Li-Qiu Zou[1], Jie Chen[2], Liang Pan[2], Jin-Zhao Jiang[3], Wei Xing[2]

[1]Department of Radiology, Peking University Shenzhen Hospital, Shenzhen, Guangdong 518036, China
[2]Department of Radiology, Affiliated Third Hospital of Suzhou University, Changzhou, Jiangsu 213003, China
[3]Department of Radiology, Hong Kong University Shenzhen Hospital, Shenzhen, Guangdong 518053, China

Abstract

Background: To compare the diagnostic values of magnetic resonance elastography (MRE) and diffusion-weighted imaging (DWI) in staging hepatic fibrosis (HF) in an animal model.

Methods: This study consisted of 44 rabbits served as HF group and 9 normal rabbits. HF group was divided into two subgroups: Group A ($n = 32$) and Group B ($n = 12$). Rabbits in Group B were served as a complementary group when rabbits in Group A suddenly died during the study. Rabbits from control and Group A underwent abdominal MR imaging (MRI), MRE, and DWI. In Group A, random eight rabbits underwent MRI examinations at 4, 5, 6, 10 weeks after carbon tetrachloride oil subcutaneous injection. Liver stiffness (LS) and apparent diffusion coefficient (ADC) values of liver parenchyma were measured. The diagnostic performance of MRE and DWI for staging HF was compared using the receiver operating characteristic curve analysis on the basis of the histopathological analysis of HF.

Results: Significant differences of LS and DWI values were present among HF stages ($P < 0.005$). The LS values measured on MRE ($r = 0.838$, $P < 0.001$) were more strongly correlated with the HF stages than with ADC values ($r = -0.527$, $P < 0.001$). The area under the receiver operating characteristic curve values of LS were significantly larger than those of DWI were for discriminating two stages of HF (0.979 vs. 0.712 for $\geq$ S1, 0.922 vs. 0.699 for $\geq$ S2). MRE showed higher specificity for predicting all stages of HF compared to DWI.

Conclusions: MRE more strongly correlated with the HF stages than DWI and is more specific in predicting all HF stages.

Key words: Diffusion-weighted Imaging; Hepatic Fibrosis; Liver Stiffness; Magnetic Resonance Elastography; Stage

INTRODUCTION

Hepatic fibrosis (HF) is the deposition of excess extracellular matrix that is rich in collagen, proteoglycans, and other macromolecules.[1] The most common causes of HF include viral infections, alcoholic and nonalcoholic steatohepatitis, toxic substances intake, metabolic disorders, and so on.[2] Fibrosis leads to end-stage cirrhosis and hepatocellular carcinoma, which are the most common causes of morbidity and mortality in developed countries.[3,4] HF can be classified into discrete stages with a variety of scoring systems.[5] The different stages of HF influence treatment decisions. Early detection and evaluation of HF are very important.

Magnetic resonance imaging (MRI) is a noninvasive tool and provides some additional functional approaches to grade HF. The common functional methods, which have been used in HF studies, include MR elastography (MRE), diffusion-weighted imaging (DWI), dynamic contrast-enhanced MRI, and so on. Among these methods, MRE is a promising technique used for quantitatively assessing the stiffness of the liver, using propagating mechanical shear waves. The mechanical properties of tissues can correlate with the extent of HF. In recent studies, MRE has been shown to be useful for staging HF with its high reproducibility and favorable diagnostic ability.[6-11] On the other hand, DWI is a fast, noninvasive imaging technique which can offer the valuable information to differentiate normal tissue from anomalous lesions at a cellular level. Some prior studies have demonstrated that the apparent diffusion coefficient (ADC) value of hepatic parenchyma is a promising biomarker in identifying moderate to severe fibrosis.[12-14] Our study was aimed to compare the sensitivity and specificity of MRE and DWI for staging HF in an animal model.

METHODS

Animal model

All studies were conducted with the approval of the Animal Care Committee at our institute. The experiments were conducted on 53 healthy New Zealand white

Address for correspondence: Prof. Wei Xing, Department of Radiology, Affiliated Third Hospital of Suzhou University, Changzhou, Jiangsu 213003, China
E-Mail: suzhxingwei@sina.cn

rabbits (weighing 2.0–2.5 kg). All rabbits were divided into two groups: Control group ($n = 9$) and HF group ($n = 44$). In addition, the HF group was divided into two subgroups: Group A ($n = 32$) and Group B ($n = 12$). If rabbits from Group A died during the experiment, the rabbits from Group B would be used to meet the shortage of Group A. HF was induced by subcutaneous injection of 50% carbon tetrachloride (CCl_4) oil once a week. The dose of CCl_4 was gradually increased (0.1 mL/kg at week 1–3; 0.2 mL/kg at week 4–6; 0.3 mL/kg at week 7–10).

Each rabbit in the control group and Group A underwent MRI examinations. In Group A, MRI examinations were performed in random eight rabbits at 4, 5, 6, 10 weeks, respectively, after first injection. After MRI examination, these animals were sacrificed for histological analysis.

Magnetic resonance examination

All examinations were performed on a 3.0T scanner (Siemens, Erlangen, Germany) by use of an 18-channel phased array knee coil. The imaging protocol included an axial T1-weighted FLASH sequence (repetition time [TR]/echo time [TE], 165/2.9 ms; field of view (FOV), 140 mm × 160 mm; matrix size, 168 × 256; slice thickness, 5 mm; gap 1 mm; bandwidth, 310 Hz/pixel), and an axial T2-weighted haste sequence (TR/TE, 1000/92 ms; FOV, 160 mm × 160 mm; matrix size, 134 × 192; section thickness, 5 mm; gap 1 mm; bandwidth, 355 Hz/pixel).

Magnetic resonance elastography

The acoustic driver system for MRE developed by Mayo Clinic was used for this study. All the rabbits were imaged in the supine position with an 8 cm-diameter, 1.5 cm-thick, cylindrical passive longitudinal shear wave driver. The center of the driver was placed on the xiphoid. The active driver generated 60 Hz shear waves in the liver during imaging. A two-dimensional (2D) gradient echo sequence was used to collect axial wave images. The parameters of the MRE gradient echo sequence were as follows: TR/TE, 50/22.7 ms; flip angle, 30°; FOV, 130 mm × 160 mm; matrix size, 128 × 84; slice thickness, 5 mm. MRE was generated by processing the acquired images of propagating shear waves with a 2D multi-scale direct inversion algorithm. Two MRE slices were obtained for each rabbit.

Diffusion-weighted imaging

Diffusion-weighted images were acquired in the transverse plane using a spin-echo echo-planar imaging sequence with diffusion-gradient encoding in three orthogonal directions. The parameters were as follows: TR 3000 ms, TE 67 ms, FOV 180 mm × 136 mm, matri × 98 × 56, section thickness 5 mm, gap 1 mm, and b values of 50, and 800 s/mm^2. The ADCs were calculated according to the formula ADC = $(\ln [SI_1/SI_2])/(b_2 - b_1)$, where SI_1 and SI_2 are signal intensities by sequence S_1 and S_2, b_1 (=50) and b_2 (=800) are gradient factors of sequences S_1 and S_2, respectively. ADC maps were automatically calculated inline on a pixel-by-pixel basis with incorporated software on a commercial workstation (Syngo; Siemens Healthcare, Erlangen, Germany).

Imaging analysis

One experienced radiologist (15 years of experience in abdominal MRI) evaluated all MRI on a commercial workstation (Syngo, Siemens Healthcare, Erlangen, Germany), who was blinded to the histopathological results.

In order to measure liver stiffness (LS) values of the hepatic parenchyma, three round-shaped (2–3 cm in diameter) regions of interest (ROI) were placed in liver on the elastogram map referring to T1-weighted image, avoiding major hepatic vessels and branches, large bile ducts, liver edges, and motion artifacts. The average LS values (in kPa) were calculated as the mean value of ROIs.

Diffusion-weighted imaging and ADC maps were evaluated on the workstation. Referring to T2-weighted image, three circular ROI were, respectively, placed in the hepatic parenchyma, avoiding vessels, large bile ducts, liver edges, and motion artifacts. The area of each ROI was set approximately 1 cm^2. The mean ADC values were calculated as the mean value of the total three ADC measurements obtained.

Histopathological examination

An experienced pathologist with 8 years of experience in histologic analysis prepared the samples and performed the histologic analysis, who was blinded to the information of the animal model establishment. The liver tissues were infiltrated with 10% formalin for fixation and embedded with paraffin. The serial 5 μm-thick sections were cut and then were stained with hematoxylin and eosin.

Fibrosis stages were assessed using the Scheuer scoring system on a scale of S0 to S4 as follows: S0, no fibrosis; S1, portal fibrosis without septa; S2, portal fibrosis with few septa; S3, numerous septa without cirrhosis; and S4, cirrhosis.[15]

Statistical analysis

Statistical analysis was performed using SPSS (version 16.0; SPSS, Chicago, IL, USA) and MedCalc (version 11.4.2.0; MedCalc for Windows, Mariakerke, Belgium). One-way analysis of variance was used to evaluate the difference in LS and ADC values at different HF stages. Correlations among LS, ADC values, the Scheuer score were assessed using the Spearman rank correlation. Receiver operating characteristics (ROCs) analysis was performed to compare the diagnostic value of MRE and DWI. In order to evaluate diagnostic values of MRE and DWI by ROC analysis, all animals were divided into some various stage grouping as follows: S0:S1-2-3-4 (≥S1), S0-1:S2-3-4 (≥S2), S0-1-2:S3-4 (≥S3), and S0-1-2-3:S4 (S4). The areas under the ROC curves (AUCs) for LS and ADC values used for staging HF were compared. A difference of $P < 0.05$ was considered significant.

RESULTS

Subjects

Two rabbits in Group A and three rabbits in Group B accidentally died. Nine rabbits had a Scheuer score of S0; 8, a score of S1; 8, a score of S2; 8, a score of S3; and 8, a score of S4.

Magnetic resonance elastography

The mean LS values of HF stages were 1.023 ± 0.13 kPa (S0), 1.334 ± 0.24 kPa (S1), 1.405 ± 0.16 kPa (S2), 2.004 ± 0.50 kPa (S3) and 1.986 ± 0.44 kPa (S4). The mean LS value increased, along with the increasing HF stage [Figure 1]. Significant differences of LS values were present among HF stages ($F = 14.665$, $P < 0.005$) [Figure 2]. No significant differences of LS values were present between S0 and S1 ($P > 0.05$), S1 and S2 ($P > 0.5$), and S3 and S4 ($P > 0.5$). The LS values significantly correlated with the extent of HF ($r = 0.838$, $P < 0.001$) [Figure 3].

Diffusion-weighted imaging

The mean ADC values of HF stages were $(1.392 \pm 0.29) \times 10^{-3}$ mm^2/s (S0), $(1.247 \pm 0.27) \times 10^{-3}$ mm^2/s (S1), $(1.381 \pm 0.29) \times 10^{-3}$ mm^2/s (S2), $(1.032 \pm 0.20) \times 10^{-3}$ mm^2/s (S3) and $(0.932 \pm 0.23) \times 10^{-3}$ mm^2/s (S4). The 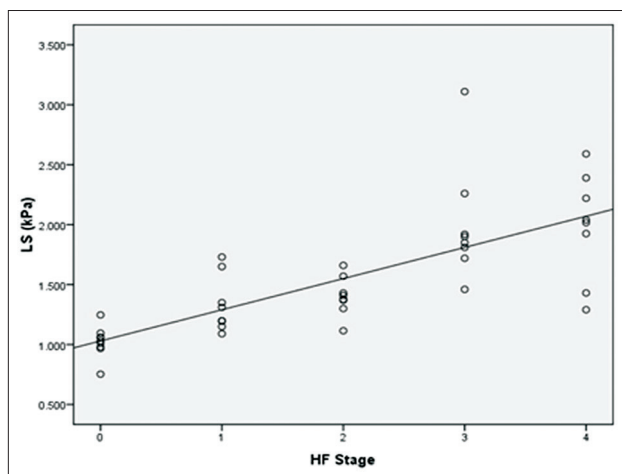mean ADC value decreased, along with the increasing HF stage [Figure 4]. Significant differences of ADC values were present among HF stages ($F = 5.344$, $P < 0.005$) [Figure 5]. No significant differences of ADC values were present among S0, S1, and S2 ($P > 0.1$). There was also no significant difference of ADC values between S1 and S3 ($P > 0.1$) and S3 and S4 ($P > 0.1$). The ADC values significantly correlated with the HF stages ($r = -0.527$, $P < 0.001$) [Figure 6].

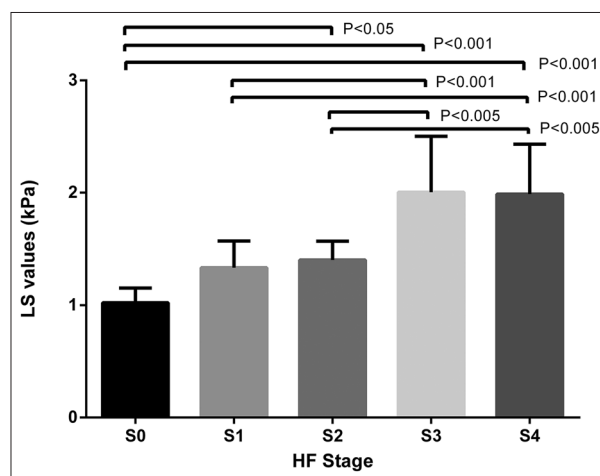## Receiver operating characteristic analysis

The areas under ROC curve for LS values were greater than those for the ADC values in all HF stages (0.979 vs. 0.712 for $\geq$ S1, 0.922 vs. 0.699 for $\geq$ S2, 0.949 vs. 0.867 for $\geq$ S3, and 0.843 vs. 0.795 for S4) [Figure 7]. But no significant differences of AUCs for LS values and ADC values were present in two groups ($\geq$ S3 and S4). The cut-off values of LS and ADC values in all stage grouping were listed in Tables 1 and 2.
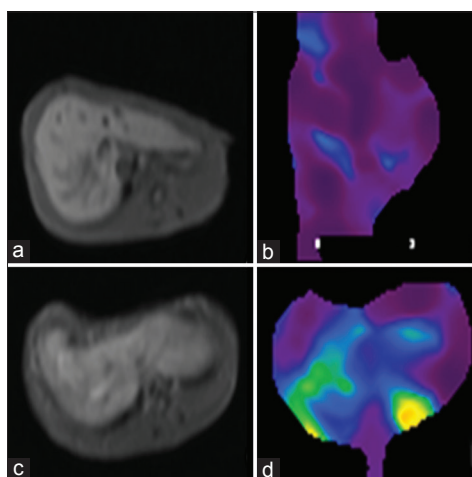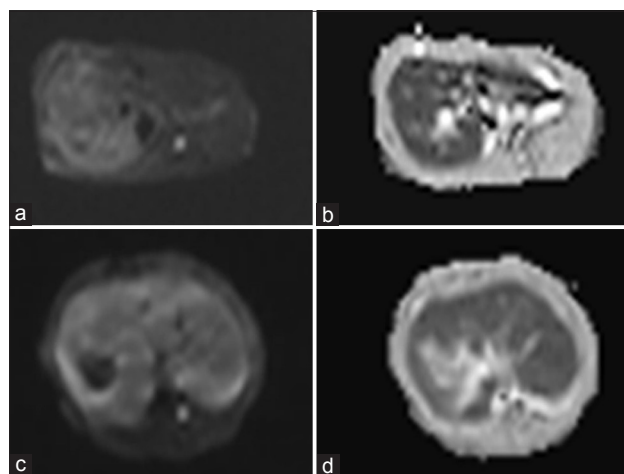

Figure 1: T1-weighted image (a and c) and magnetic resonance elastography (b and d) of two rabbits with hepatic fibrosis (HF). One rabbit in the top row with mild HF (S2) shows mean LS value of 1.66 kPa, whereas the other (S4) in the lower row has significantly elevated liver stiffness (mean liver stiffness value = 2.59 kPa).

Figure 2: The plot shows the significant differences of liver stiffness values among all hepatic fibrosis stages except for S0 versus S1, S1 versus S2, and S3 versus S4.


Figure 3: Scatterplot shows the relationship between the liver stiffness (LS) value and hepatic fibrosis (HF) stages. The LS values significantly correlated with HF stages ($r = 0.838$, $P < 0.001$).

Figure 4: Diffusion-weighted imaging (a and c) and apparent diffusion coefficient (ADC) (b and d) maps of two rabbits with hepatic fibrosis (HF). One rabbit in the top row with mild HF (S2) shows mean ADC value of 1.216×10^{-3} mm^2/s, whereas the other (S4) in the lower row has significantly decreased ADC values (mean ADC value = 0.757×10^{-3} mm^2/s).
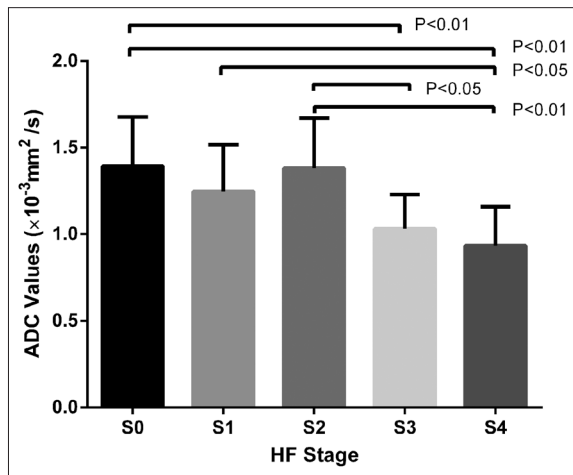
Figure 5: The plot shows significant differences of apparent diffusion coefficient values between S0 and S3, S0 and S4, S1 and S4, S2 and S3, and S2 and S4.

Figure 6: Scatterplot shows the relationship between the apparent diffusion coefficient (ADC) value and hepatic fibrosis (HF) stages. The ADC values significantly correlated with HF stages ($r = -0.527, P < 0.001$).

DISCUSSION

In this study, our results demonstrated that there was a significant difference of LS and ADC values among HF stages in a rabbit model. The LS values measured on MRE were more strongly correlated with the HF stages than with ADC values. MRE showed higher specificity for predicting all stages of HF compared with DWI. But No significant difference of the diagnostic performances of MRE and DWI in two groups ($\geq$S3 and S4) were present.

Up to now, there are five system of scoring HF, including Knodell HAI, the Scheuer scoring system, Ishak's system, Metavir system, and Ishak modified HAI.[16] The Scheuer scoring system can be applied for chronic viral hepatitis as well as nonviral hepatitis. In this present study, the animal model was induced by CCl_4. So the Scheuer scoring system was used to evaluate HF stages. In term of this system, the portal and lobular components in HF were given equal weightage. The periportal and portal lesions were classified into a single category.

Magnetic resonance elastography can evaluate the tissue stiffness using propagating shear waves.[17] The speeds of propagation in tissues are influenced by the difference of tissue stiffness. The LS value becomes larger, along with increasing the tissue stiffness.[18] On the elastograms of HF, the normal hepatic parenchyma shows blue. With the increase of LS, the hepatic parenchyma gradually shows green, yellow, and even red.[19] MRE has been used to assess HF caused by various etiologies.[7,9,20] In a prior study, Yin *et al.* reported there was a linear correlation between LS and fibrosis extent in an animal model.[8] In our study, MRE also showed a good correlation with HF staging. This result indicated that the LS values measured on MRE can be used to represent the architectural distortion in HF.

Signal properties on DWI reflect the microstructure and the physiologic state of tissues.[21] Stiffer of liver parenchyma, the ADC values of hepatic parenchyma are lower.[22] Annet
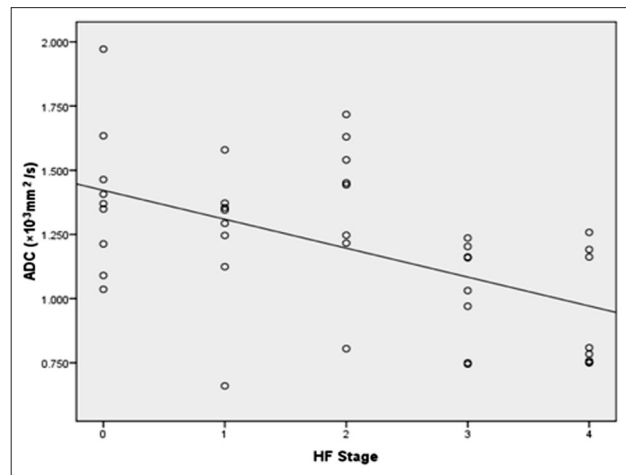
Table 1: Diagnostic value of LS values at different HF stages

| Items	≥S1	≥S2	≥S3	S4
Cut-off value	1.095	1.350	1.660	1.920
Sensitivity (%)	96.87	87.50	81.25	75.00
Specificity (%)	88.89	88.24	96.00	93.94
Positive predictive value (%)	96.9	91.30	92.90	71.40
Negative predictive value (%)	88.9	83.30	88.90	91.20

LS: Liver stiffness; HF: Hepatic fibrosis.

Table 2: Diagnostic value of ADC values at different HF stages

Items	≥S1	≥S2	≥S3	S4
Cut-off value	1.345	1.258	1.203	1.191
Sensitivity (%)	75.00	79.17	87.50	87.50
Specificity (%)	55.56	58.82	80.00	66.67
Positive predictive value (%)	85.70	73.1	73.70	38.90
Negative predictive value (%)	38.50	66.7	90.90	95.70

ADC: Apparent diffusion coefficient; HF: Hepatic fibrosis.

et al. demonstrated that the ADC of the live rats correlated with the severity of HF.[23] Our results also explored that significant differences of ADC values were also present among HF stages, and ADC values significantly correlated with HF stages. ADC measurements are influenced by collagen deposition and perfusion. The b-value is a very important factor, which influences the contribution of microperfusion in ADC measurements. Ozkurt *et al.* recommended that a *b*-value of 750 s/mm^2 or greater can help quantify liver fibrosis accurately.[24] In this present study, large b value ($b = 800$ s/mm^2) was used to decrease the component of microperfusion. Thus, these correlations between ADC values and HF stages in our study can be explained by extracellular accumulation of collagen, glycosaminoglycans, and proteoglycans, which can restrict water diffusion.
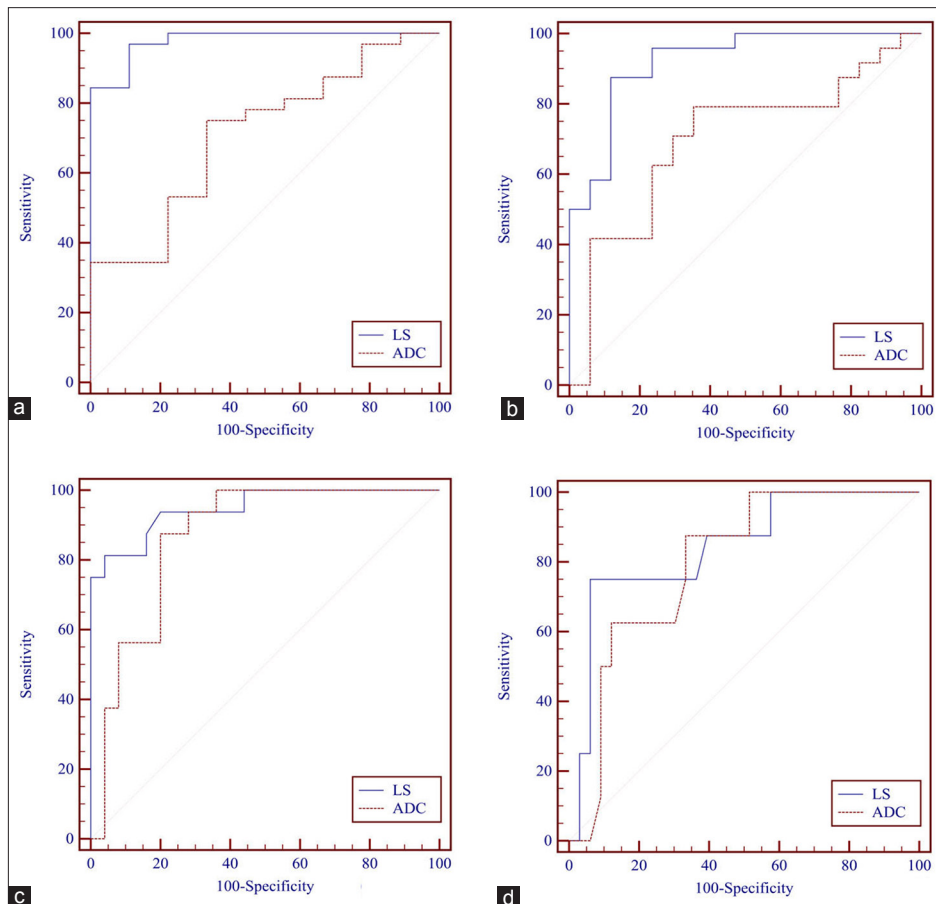
Figure 7: The receiver operating characteristic (ROC) analysis on evaluating the diagnostic value of magnetic resonance elastography and diffusion-weighted imaging (≥S1,A;≥S2,B;≥S3,C;S4,D). The areas under ROC curve for liver stiffness values were greater than those for the apparent diffusion coefficient values in all hepatic fibrosis stages (≥S1, 0.922 vs. 0.699 for ≥S2, 0.949 vs. 0.867 for ≥S3, and 0.843 vs. 0.795 for S4).

In a recent meta-analysis on evaluating performance of MRE and DWI for staging HF, the sensitivity, specificity, and AUC of MRE for staging F0–F1 versus F2–F4 and F0–F2 versus F3–F4 were higher accuracy than those of DWI.[25] Wang *et al*. compared the ability of MRE and DWI for staging HF in patients with chronic hepatitis.[26] In his study, MRE showed greater capability than DWI in discriminating Stage 2 or greater (≥F2), Stage 3 or greater (≥F3), and cirrhosis (≥F4), shown as significant differences in AUC. Meanwhile, MRE showed higher sensitivity and specificity in predicting fibrosis scores ≥F2, ≥F3, and F4 than those of DWI. But the correlationship between ADC values and HF stages was not present in his study. Our results demonstrated the sensitivity, specificity, and AUC of MRE for staging ≥S1 and ≥S2 were higher than those of DWI. No significant differences of AUCs between MRE and DWI were present in staging ≥ S3 and S4 while the specificity of MRE was higher than that of DWI. This discrepancy between our result and prior studies may be caused by some factors. First, our animal model induced by CCl_4 administration other than subjects in prior studies. Second, the echo planar imaging sequence is very sensitive to magnetic susceptibility artifacts and motion artifacts, which can influence the measurements of ADC values.

Several limitations exist in our study. First, we did not dynamically measure LS values and ADC values because the rabbits with HF were not in good healthy conditions and were difficult to complete the continuous examinations. Second, we did not evaluate the influence of steatosis, iron overload, and edema on stiffness, and ADC measurements.

In conclusion, magnetic resonance elastography more strongly correlated with the HF stages than DWI and is more specific in predicting all HF stages.

References

1. Friedman SL. Hepatic fibrosis–Overview. Toxicology 2008;254:120-9.
2. Rockey DC. Hepatic fibrosis, stellate cells, and portal hypertension. Clin Liver Dis 2006;10:459-79, vii.
3. El-Serag HB. Hepatocellular carcinoma and hepatitis C in the United States. Hepatology 2002;36:S74-83.
4. Befeler AS, Di Bisceglie AM. Hepatocellular carcinoma: Diagnosis and treatment. Gastroenterology 2002;122:1609-19.
5. Brunt EM, Janney CG, Di Bisceglie AM, Neuschwander-Tetri BA, Bacon BR. Nonalcoholic steatohepatitis: A proposal for grading and staging the histological lesions. Am J Gastroenterol 1999;94:2467-74.
6. Xanthakos SA, Podberesky DJ, Serai SD, Miles L, King EC, Balistreri WF, *et al*. Use of magnetic resonance elastography to assess hepatic fibrosis in children with chronic liver disease. J Pediatr 2014;164:186-8.
7. Huwart L, Peeters F, Sinkus R, Annet L, Salameh N, ter Beek LC, *et al*. Liver fibrosis: Non-invasive assessment with MR elastography. NMR Biomed 2006;19:173-9.

8. Yin M, Woollard J, Wang X, Torres VE, Harris PC, Ward CJ, *et al.* Quantitative assessment of hepatic fibrosis in an animal model with magnetic resonance elastography. Magn Reson Med 2007;58:346-53.

9. Kim BH, Lee JM, Lee YJ, Lee KB, Suh KS, Han JK, *et al.* MR elastography for noninvasive assessment of hepatic fibrosis: Experience from a tertiary center in Asia. J Magn Reson Imaging 2011;34:1110-6.

10. Runge JH, Bohte AE, Verheij J, Terpstra V, Nederveen AJ, van Nieuwkerk KM, *et al.* Comparison of interobserver agreement of magnetic resonance elastography with histopathological staging of liver fibrosis. Abdom Imaging 2014;39:283-90.

11. Lee Yj, Lee JM, Lee JE, Lee KB, Lee ES, Yoon JH, *et al.* MR elastography for noninvasive assessment of hepatic fibrosis: Reproducibility of the examination and reproducibility and repeatability of the liver stiffness value measurement. J Magn Reson Imaging 2014;39:326-31.

12. Cece H, Ercan A, Yildiz S, Karakas E, Karakas O, Boyaci FN, *et al.* The use of DWI to assess spleen and liver quantitative ADC changes in the detection of liver fibrosis stages in chronic viral hepatitis. Eur J Radiol 2013;82:e307-12.

13. Chiaradia M, Baranes L, Pigneur F, Djabbari M, Zegai B, Brugières P, *et al.* Liver magnetic resonance diffusion weighted imaging: 2011 update. Clin Res Hepatol Gastroenterol 2011;35:539-48.

14. Sandrasegaran K, Akisik FM, Lin C, Tahir B, Rajan J, Saxena R, *et al.* Value of diffusion-weighted MRI for assessing liver fibrosis and cirrhosis. AJR Am J Roentgenol 2009;193:1556-60.

15. Scheuer PJ. Classification of chronic viral hepatitis: A need for reassessment. J Hepatol 1991;13:372-4.

16. Mannan R, Misra V, Misra SP, Singh PA, Dwivedi M. A comparative evaluation of scoring systems for assessing necro-inflammatory activity and fibrosis in liver biopsies of patients with chronic viral hepatitis. J Clin Diagn Res 2014;8:FC08-12.

17. Muthupillai R, Lomas DJ, Rossman PJ, Greenleaf JF, Manduca A, Ehman RL. Magnetic resonance elastography by direct visualization of propagating acoustic strain waves. Science 1995;269:1854-7.

18. Venkatesh SK, Yin M, Ehman RL. Magnetic resonance elastography of liver: Technique, analysis, and clinical applications. J Magn Reson Imaging 2013;37:544-55.

19. Shi Yu, Guo QY, Zhang L, Xia F, Yu B. MR elastography on 3.0T scanner: A preliminary study of liver stiffness measured and interrater consistency in volunteers and patients with chronic liver disease. Chin J Radiol 2013;47:1005-8.

20. Lee JE, Lee JM, Lee KB, Yoon JH, Shin CI, Han JK, *et al.* Noninvasive assessment of hepatic fibrosis in patients with chronic hepatitis B viral infection using magnetic resonance elastography. Korean J Radiol 2014;15:210-7.

21. Chen J, Sheng J, Xing W, Aoun H, Chen M, Bi HL, *et al.* Monitoring early response of lymph node metastases to radiotherapy in animal models: Diffusion-weighted imaging vs. morphological MR imaging. Acta Radiol 2011;52:989-94.

22. Shi Y, Guo QY, Liao W, Ma Y, Qi WX. MR diffusion weighted imaging for quantification of liver fibrosis in patients with chronic viral hepatitis. Chin J Radiol 2010;44:65-9.

23. Annet L, Peeters F, Abarca-Quinones J, Leclercq I, Moulin P, Van Beers BE. Assessment of diffusion-weighted MR imaging in liver fibrosis. J Magn Reson Imaging 2007;25:122-8.

24. Ozkurt H, Keskiner F, Karatag O, Alkim C, Erturk SM, Basak M. Diffusion weighted MRI for hepatic fibrosis: Impact of b-value. Iran J Radiol 2014;11:e3555.

25. Wang QB, Zhu H, Liu HL, Zhang B. Performance of magnetic resonance elastography and diffusion-weighted imaging for the staging of hepatic fibrosis: A meta-analysis. Hepatology 2012;56:239-47.

26. Wang Y, Ganger DR, Levitsky J, Sternick LA, McCarthy RJ, Chen ZE, *et al.* Assessment of chronic hepatitis and fibrosis: Comparison of MR elastography and diffusion-weighted imaging. AJR Am J Roentgenol 2011;196:553-61.